

Update on the IsoDAR 60 MeV/amu Cyclotron Acceleration Simulations

Daniel Winklehner*
for the DAE δ ALUS Collaboration

(Dated: February 19, 2022)

In this technical report, the work done by members of the DAE δ ALUS collaboration on simulating the acceleration of 5 mA of H_2^+ in the IsoDAR compact isochronous cyclotron is summarized. The findings are that sufficient turn separation between the $(N - 1)^{\text{th}}$ and N^{th} turn can be achieved with either initially matched but also with mismatched beams by careful placement of collimators to scrape away halo particles before the beam energy has reached 2 MeV/amu. Here we define "sufficient" as < 200 W beam loss on the septum. In the acceleration simulations, beam losses on the collimators vary from 10% to 25% depending on the initial beam conditions. The collimator placement in the central region, halo formation, and turn separation at the final turn are discussed. Finally, a scheme to further mitigate the risk of beam loss on the extraction septum by placing a narrow stripping foil in front of it is investigated. We also present the findings of a separate study subcontracted to the company AIMA, who investigated injection of H_2^+ ions through a spiral inflector and accelerating them for four turns. Here the reported beam loss before 2 MeV/amu was 58%, but bunches were not accelerated further, so we are not reporting this as a final result.

I INTRODUCTION

A 10 mA 60 MeV/amu cyclotron would have enormous impact in neutrino physics through the IsoDAR project [1–3], for isotope production [4–6], and as a pre-accelerator for a 10 mA, 800 MeV - 1 GeV cyclotron that can be used for ADS(R) [7–10] and particle physics, including the DAE δ ALUS experiment [11–15]. Potential uses are summarized in Table I. Because this concept originated within the development of DAE δ ALUS, this multi-use 60 MeV/amu cyclotron is historically called the DAE δ ALUS Injector Cyclotron, or DIC. Here we use the terms *IsoDAR cyclotron* and *DIC* interchangeably.

Among the challenges for the DIC are the strong space charge effects of such a high intensity beam and the small phase acceptance window of the isochronous cyclotron. Space charge matters most in the Low Energy Beam Transport Line (LEBT) and during injection into the cyclotron. Our concept to mitigate these risks is based on three novelties: 1. Accelerating 5 mA of H_2^+ instead of 10 mA of protons, leading to the same number of nucleons on target at half the electrical current as the remaining electron bound in the H_2^+ molecular ion reduces the electrical current in the beam. 2. Injecting into the compact cyclotron via an RFQ partially embedded in the yoke to aggressively pre-bunch the beam. 3. Designing the cyclotron main acceleration to optimally utilize vortex motion. In the following subsections, the injection and central region design will be briefly summarized. In Section II, the previously published and new unpublished work by collaboration members will be presented and reviewed. Finally, the implications for IsoDAR and further mitigation methods for beam loss on the extraction septum, using a stripping foil placed right before the septum will be discussed in Section III.

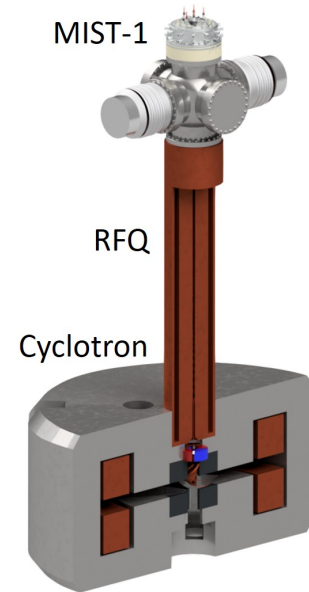


FIG. 1. Cartoon rendering of the RFQ Direct Injection Prototype. Ions are produced in the ion source (top), are accelerated and bunched in the RFQ (middle) and injected into the cyclotron central region to be accelerated to 1 MeV/amu (bottom).

A. Injection

In order to accelerate H_2^+ , it has to be produced in an ion source in sufficient quantities. At MIT, we have built a prototype ion source optimized for H_2^+ production: MIST-1. For a description, see our recent publication on high intensity cyclotrons [16] and references therein. Systematic studies are ongoing and a publication about the performance of the source is forthcoming. The ion source design is based on a previous multicusp ion source developed at LBNL, which reported a

* winklehn@mit.edu

TABLE I. A few potential uses for high current proton beams and how cyclotrons can be leveraged to reach the goals. ADSR: Accelerator Driven Sub-critical Reactors, ADS: Accelerator Driven Systems for nuclear waste transmutation. Cyclotrons can be a cost-effective alternative for tests and demonstrations at the low-power end of the spectrum (tens of mA). Adapted from [16].

Application	Field	Current	Energy	Comment
IsoDAR [1–3]	neutrinos	10 mA	60 MeV	Use $\bar{\nu}_e$ from decay-at-rest to search for sterile neutrinos.
DAE δ ALUS [11–15]	neutrinos	10 mA	800 MeV	A proposed search for CP violation in the neutrino sector.
ADSR [7, 8]	energy	10-40 mA	~ 1 GeV	Cyclotrons are a cost-effective alternative for demonstrator experiments.
ADS [9, 10]	energy	4-120 mA	~ 1 GeV	Cyclotrons are a cost-effective alternative for demonstrator experiments.
Isotopes [4–6]	medicine	1 – 10 mA	3-70 MeV	E.g.: 10 mA/60 MeV can increase worldwide ^{225}Ac production by 6000 [5].
Material testing	fusion	10-100 mA	5-40 MeV	Testing of fusion materials similar to IFMIF [17], at lower power.

ratio of 20% protons and 80% H_2^+ , as well as a maximum beam density of 50 mA/cm² [18]. The maximum beam density from MIST-1 so far was 40 mA/cm², and the best H_2^+ fraction was seen at 25 mA/cm², with 20% p⁺, 20% H_2^+ , 50% H_3^+ and 10% H_2O^+ (unpublished). As commissioning of MIST-1 is ongoing, we are using the 80% H_2^+ reported in [18] for all simulations. In Ref. [16], we also describe the physics design of an RFQ linear accelerator-buncher which is going to be embedded in the cyclotron yoke and will deliver a highly bunched beam to the spiral inflector – an electrostatic device that bends the beam from the axial direction into the acceleration plane of the cyclotron (median plane, or mid-plane), where the beam is accelerated and matched to the cyclotron main acceleration (described in Section II). A prototype of this *RFQ Direct Injection Project (RFQ-DIP)* is currently under construction (see Figure 1 for a cartoon rendering). By aggressively pre-bunching the beam, we fit more particles into the RF phase acceptance window of $\approx 20^\circ$. Due to the high bunching factor and strong space charge, the beam starts diverging in transverse direction and de-bunching in longitudinal direction soon after the exit of the RFQ. To mitigate this, a re-bunching cell has been included in the RFQ design and an electrostatic quadrupole focusing element has been placed before the spiral inflector. In addition, the spiral

inflector electrodes can be carefully shaped to add vertical focusing as well. Transmission from the ion source to the exit of the spiral inflector was $\approx 78\%$ for both test cases (10 mA and 20 mA of total beam current, 20% protons, 80% H_2^+) with transverse emittances of 0.3–0.4 mm-mrad (1-RMS, normalized) and 7–8 keV/amu-ns longitudinal emittance (1-RMS) [16].

B. Central region

Particle distributions obtained in the injection simulations were used in a detailed central region study subcontracted to the company AIMA Developpement in France and comulated in a technical report [19]. In this study, a 3D magnetic field was generated that includes the effects of vanadium-permendum (VP) inserts in the pole tips and one poletip cut short to allow placement of the spiral inflector (see Figure 2). The VP has a sharper turn in the B-H curve, slightly improving the flutter in the central region. An optimized dee electrode system was generated during the study, which can be seen in Figure 3. This system exhibits good vertical focusing and small orbit center precession. The dee peak voltage was increased to 80 kV from the nominal 70 kV in the IsoDAR baseline, which is still tolerable. By placing a single collimator in the first turn, the desired edge-to-edge turn separation of 1 cm was achieved during the fourth turn

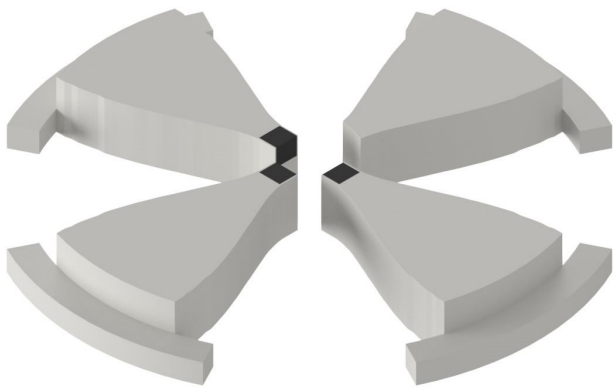


FIG. 2. CAD rendering of the iron poles for magnetic field calculations (lower half only). The vanadium-permendum inserts can be seen in black at the pole tips. One of the pole tips is truncated, yielding space for the spiral inflector.

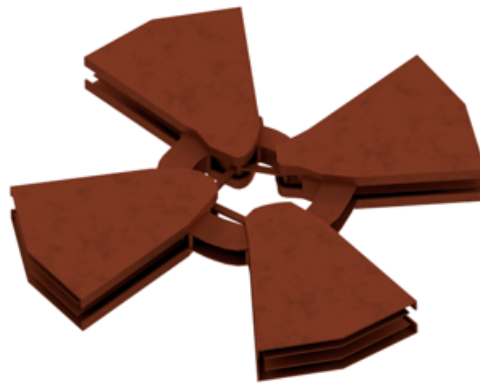


FIG. 3. CAD rendering of the dee-dummydee electrodes, posts and additional grounded elements, used to calculate the electric fields in the cyclotron central region.

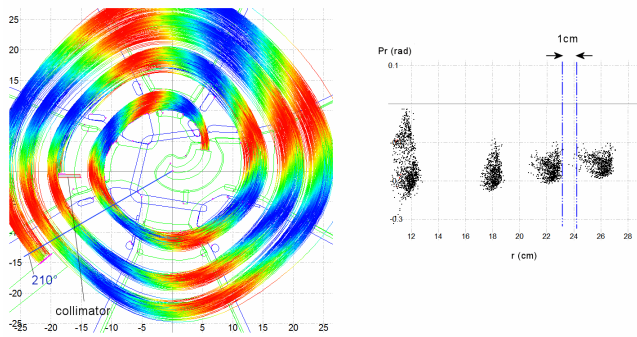


FIG. 4. Left: Trajectories of the first 3.5 turns (2 MeV) in the simulated central region. Right: Demonstrated turn separation of 1 cm (edge-to-edge) after placing a collimator in the first turn. Beam transmission from the entrance of the spiral inflector to the probe was 42%. From [19].

(at 1 MeV/amu beam energy). This led to a beam loss of 58% in spiral inflector and central region and a cumulative transmission efficiency of 42%. Note that this replaces the 78% presented in the previous subsection as AIMA used their own spiral inflector model. As no additional significant losses are anticipated in acceleration and extraction, in order to obtain 5 mA of beam, about 12 mA H_2^+ need to be injected into the RFQ. Assuming 80% H_2^+ , we are looking at a total extracted current of 15 mA. RFQ simulations have shown that we can get good results up to 20 mA with the current design [16]. However, this central region study, as of yet, does not include space charge effects (space charge was included up to the entrance of the spiral inflector). Inclusion of space charge will change the beam dynamics (vortex-effect). Furthermore, collimator placement is restricted to one location. Other studies (see Section II) suggest that better results can be obtained with multiple collimators in the first 3-4 turns. Both, space charge and collimator placement, will be investigated further.

II SIMULATIONS OF THE ISODAR MAIN ACCELERATION

The simulations of the IsoDAR main acceleration were done in three steps: In 2013, Jianjun Yang performed a set of studies for the 60 MeV/amu DAE δ ALUS Injector Cyclotron (DIC), which later became the IsoDAR cyclotron, and the 800 MeV/amu DAE δ ALUS Superconducting Ring Cyclotron (DSRC), demonstrating that with careful collimator placement and by including neighboring bunch effects across several turns, beam loss on a 0.5 mm thick extraction septum, placed at $R = 200$ cm, could be kept below the required 200 W [21]. The starting condition was a 1.5 MeV/amu beam on the fourth turn. In 2016, Jakob Jonnerby extended these studies down to starting energies of 193 keV/amu (first turn) for his master's thesis [22]. In 2017, Maria Yampolskaya further refined the collimator placement during a summer

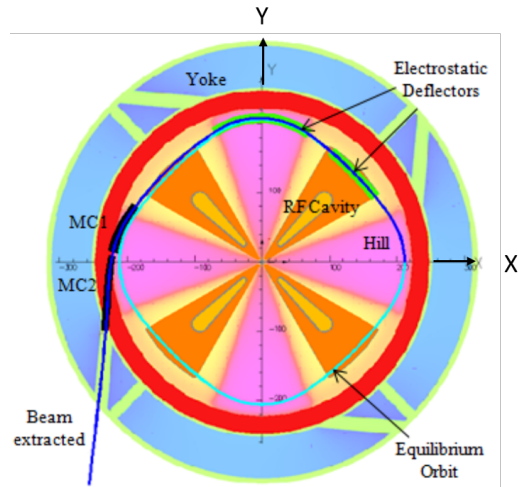


FIG. 5. Cartoon of the IsoDAR cyclotron. Indicated are the hills (magenta) and valleys (yellow) of the isochronous field, the four double-gap RF cavities (centered around 45° , 135° , 225° , and 315°), the 60 MeV/amu static equilibrium orbit, and examples of deflector and magnetic channel (MC1 and MC2) placements. The outer radius of the yoke is 3.2 m. From [20].

internship at MIT. An important factor in the clean extraction is the vortex effect, a combination of external focusing forces in the isochronous cyclotron and space-charge forces from the Coulomb interaction of the particles in the high intensity beam [23]. Vortex motion has first been seen in PSI Injector II and subsequently reproduced with simulations in a previous publication [24]. All simulations in this section were performed using the well-established parallel particle-in-cell code OPAL that takes into account space charge [25]. A top-down view of the IsoDAR cyclotron is shown in Figure 5. In harmonic mode 6, the opening angle of the cavities was chosen to be 28° . Example placements of electrostatic deflectors (with septum) can be seen as well. All azimuthal angles in this section are measured from -180° to 180° , with 0° the positive x-axis.

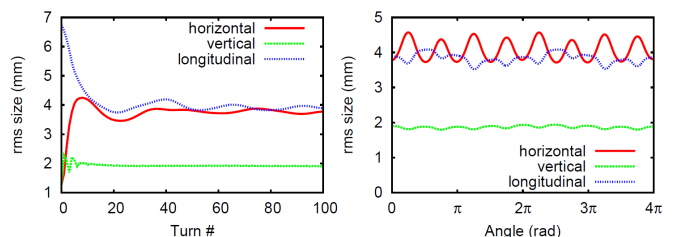


FIG. 6. The rms size snapshot at 0° azimuth in 100 turns (left), and the rms envelope in the last two turns (right), for a coasting (unaccelerated) beam with 5 mA and 1.5 MeV/amu. This demonstrates the formation of a stationary (matched) distribution from an initially unmatched beam. From [21].

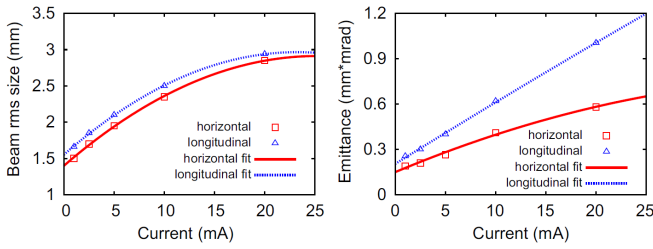


FIG. 7. Stationary rms beam size (left) and normalized rms emittance (right) vs. beam current. From [21].

A. Early simulations starting at 1.5 MeV/amu

In this subsection, Jianjun's work from 2013 [21] is summarized.

1. Matched coasting beam

To demonstrate the formation of a stable matched distribution, a coasting beam was first tracked for 100 turns without acceleration in the IsoDAR cyclotron nominal magnetic field. The initial beam was Gaussian and had rms beam sizes of 1.26 mm in transverse and 6.7 mm in longitudinal direction (corresponding to 40° full phase width). In Figure 6, the results are shown, demonstrating the formation of a matched beam of 4 mm rms size within ≈ 20 turns. The beam size then oscillates with the number of sectors (Figure 6, right). Stationary rms beam size and normalized rms emittance are plotted vs different beam currents in Figure 7. It can be concluded that no flattop cavity is necessary and all four valleys can be used for accelerating dee-dummydee structures, yielding high energy gain per turn and hence higher turn separation at extraction.

2. Accelerated beam

The acceleration simulations in [21] start at the exit of the central region. Considering that both the space charge effects in the injection line and the transverse longitudinal coupling motion in the spiral inflector inevitably increase the emittance, the initial normalized

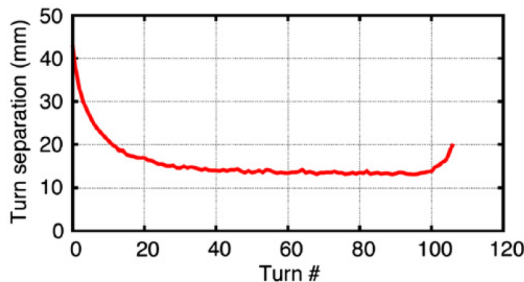


FIG. 8. Center-to-center turn separation as a function of turn number. From [21].

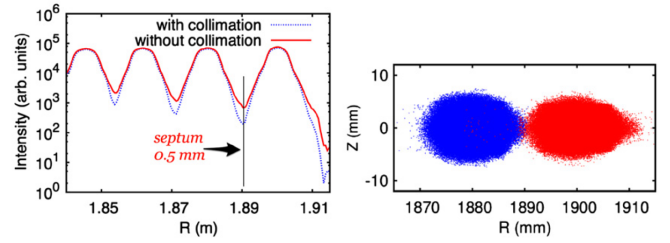


FIG. 9. The radial profile of the last four turns at the center of a valley (left) and the rz projection of the collimated particles during the last 2 turns (right) for 5mA of beam current. The total macroparticle number in a bunch is 10^6 . From [21].

emittance at the exit of central region is set to a large value compared to typical ion sources, i.e. 0.6π -mm-mrad. The phase acceptance and initial energy spread are assumed to be 10° 20° and 0.4% respectively. In order to reduce the tail particles of the extracted beam, four collimators are placed at around 1.9 MeV/amu to cut off about 10% of the halo particles. High turn separation during the final turns is achieved by a combination of the vortex effect, using the $\nu_r = 1$ resonance (sharp radial field drop), and a high energy gain per turn. In [21], the separation of the final turn is ≈ 20 mm for a 5 mA beam (see Figure 8). The turn separation is shown in Figure 9 and the loss on the septum is listed in Table II for 1, 5, and 10 mA using 10° and 20° initial phase. These simulations, while using an initial beam with higher than usual emittance and phase width to provide a safety margin, neglect the energy spread introduced by the spiral inflector, and start with a matched distribution at 0.54 MeV/amu. Ideally, the results of the central region study would be used for the main acceleration simulations. This is a work in progress, currently ongoing at MIT. However, one can also close in on the matching point of central region and main acceleration by extending the latter to lower starting energies and refining the collimator placement. This is reported in the following subsection.

B. Extension of OPAL simulations to lower starting energies

In his ETHZ master's thesis [22], Jakob Jonnerby extended the IsoDAR cyclotron simulations to a lower starting energy of 193 keV/amu and refined the collimator placement. He went through a similar process as described in the previous subsection in order to find a matched distribution. The studied collimator placements

TABLE II. Beam loss power on the 0.5 mm wide septum for 90% duty cycle. From [21].

Injection phase width	1 mA	5 mA	10 mA
10°	27 W	108 W	1080 W
20°	63 W	99 W	1422 W

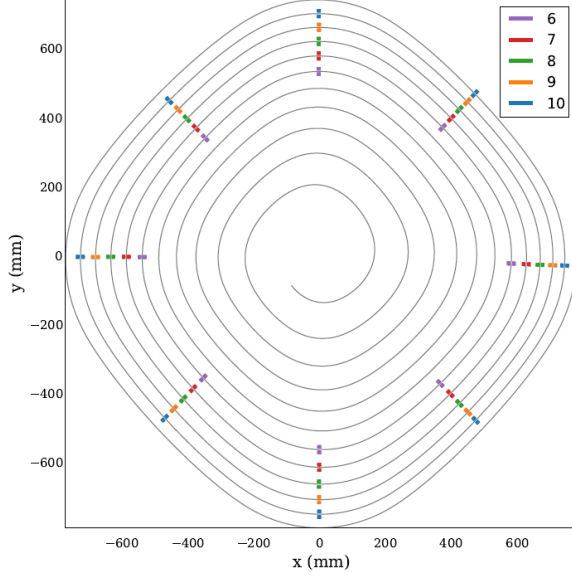


FIG. 10. Possible placements of collimators in turns 6 - 10 overlaid with the design trajectory from single particle tracking. Collimators were only placed in a single turn for each simulation. From [22].

are shown in Figure 10. The best results were obtained with collimators placed either in turn 8, 9 or 10. With the lower starting energy and different collimator placement, Jonnerby reports a turn separation at 60 MeV/amu of 15 mm center-to-center (which is lower than the 20 mm of Yang) and states that the beam power loss on the septum is larger than the limit of 200 W. The rz projection of the last two turns at an azimuthal angle of -45° is shown in Figure 11. A major difference between Jonnerby's and Yang's work is that Jonnerby ends the simulations at $r = 1.86$ m and Yang at $r = 1.9$ m. Tracking for more turns, while increasing the beam energy beyond 60 MeV/amu, would bring the beam closer to the $\nu_r = 1$ resonance region of the magnetic field, further increasing the sepa-

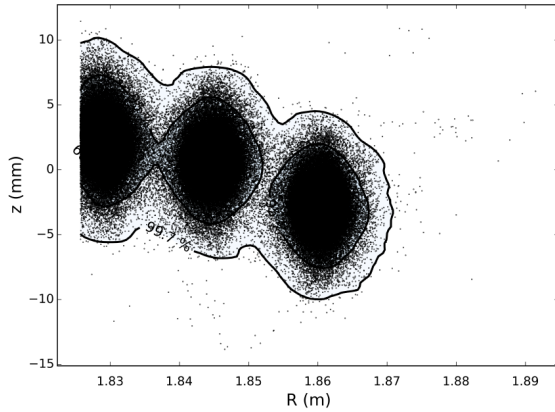


FIG. 11. The two last turns projected on the $r - z$ plane, at an azimuthal angle of -45° in the cyclotron. From [22].

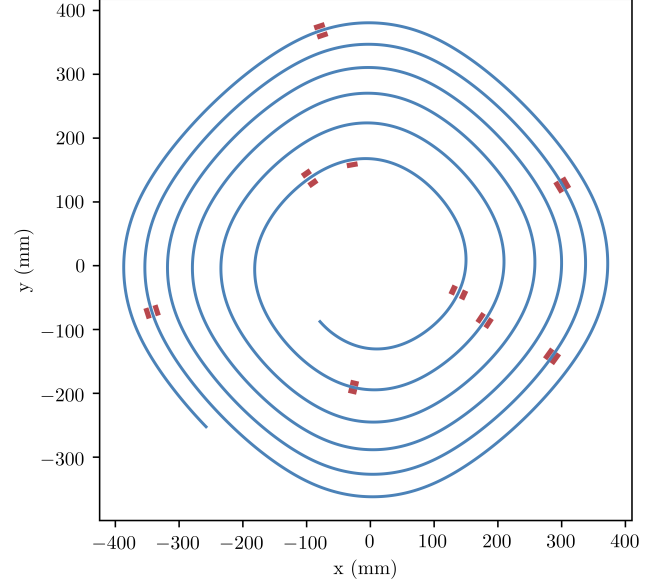


FIG. 12. The bunch centroid trajectory of the first 6 turns (blue) with 9 collimators (red).

ration at the expense of beam quality. It was shown in his work, that a matched distribution can be found at lower energy and that the beam exhibits vortex motion, stabilizing the beam growth, leading to similar beam sizes as reported by Yang. The beam loss on the collimators is $\approx 23\%$. Maria Yampolskaya, during a summer internship at MIT in 2017, refined Jonnerby's collimator placement and was able to improve the beam quality and turn separation close to extraction. DW, for this report, re-ran several of Yampolskaya's simulations, tuned the RF phases slightly, and further optimized the collimator placement. This work is, as of yet, unpublished.

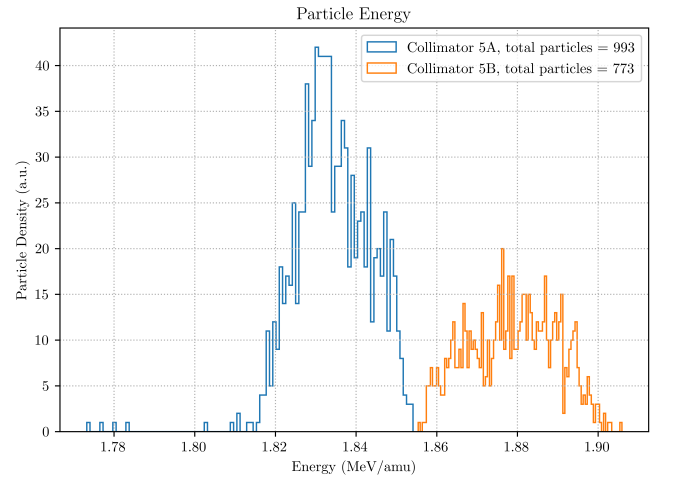


FIG. 13. Energy histogram of particles lost on collimator 9. Total number of accelerated particles = 100,000. Collimator 5A is on the inside of the orbit, Collimator 5B on the outside.

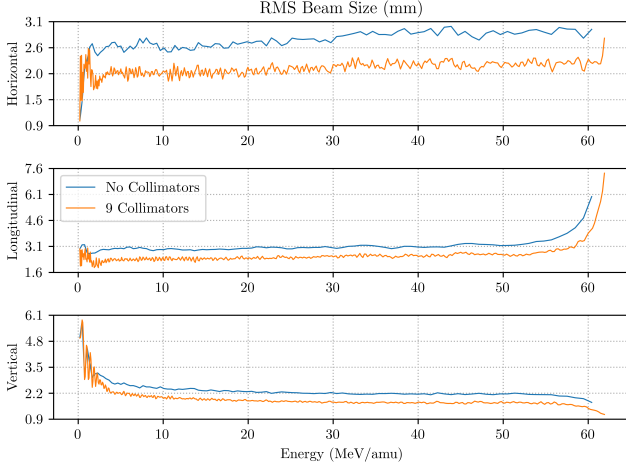


FIG. 14. RMS beam size for two cases: No collimators and 9 collimators. A clear reduction can be seen with collimators. Also visible is the effect of the $\nu_r = 1$ resonance above 60 MeV/amu. The longitudinal and radial beam size are approximately the same above 5 MeV/amu, due to the vortex effect.

The final result for simulations in harmonic mode 6, starting with a mean beam energy of 193 keV/amu and placing the bunch on a matched orbit at -135° yielded deposited beam power on the septum of 98 W. For this, 9 collimators were placed in the first 6 turns (see Figure 12). The highest energy particles lost on the collimators were ≈ 1.9 MeV/amu (cf. Figure 13), similar to Yang's choice. The RMS beam size for a case without collimators and with the 9 collimators as well as the halo parameter, defined as:

$$H = \frac{\langle x^4 \rangle}{\langle x^2 \rangle^2} - 1 \quad (1)$$

are shown in Figure 14 and Figure 15, respectively. A clear reduction of both can be seen with collimators. Also visible is the effect of the $\nu_r = 1$ resonance above 60 MeV/amu. The overall beam loss in the central region in this simulation was 27%. The deposited power on a probe, located at 30° azimuth, sorted in 0.5 mm bins (a conservative choice for septum thickness), is shown in Figure 16 (top) with an R-Z scatter plot of the particles passing through the probe (bottom). Septum placement is indicated in red. A few stray particles with higher energies are still visible, which will deposit their energy in other parts of the cyclotron, adding to activation. These are few, and can also be suppressed with further collimator optimization. These results show clearly that, even with a beam starting at 193 keV/amu (essentially during the innermost turn), collimators can be placed such that the turn separation at extraction is sufficient, albeit with beam losses around 25% in the central region.

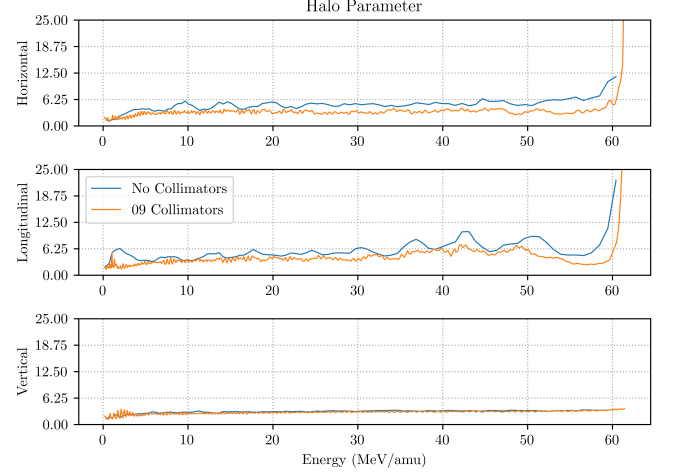


FIG. 15. Halo parameter (cf. (1)) for two cases: No collimators and 9 collimators. A clear reduction can be seen with collimators. Also visible is the effect of the $\nu_r = 1$ resonance above 60 MeV/amu.

III DISCUSSION

All 60 MeV/amu simulations point to a similar conclusion: The beam exhibits vortex motion, which generates a stable round distribution. At the same time, a halo is formed that needs to be removed by placing collimators early-on. One interesting observation is that, starting at 193 keV/amu, it seems to take ~ 4 -6 turns for this pro-

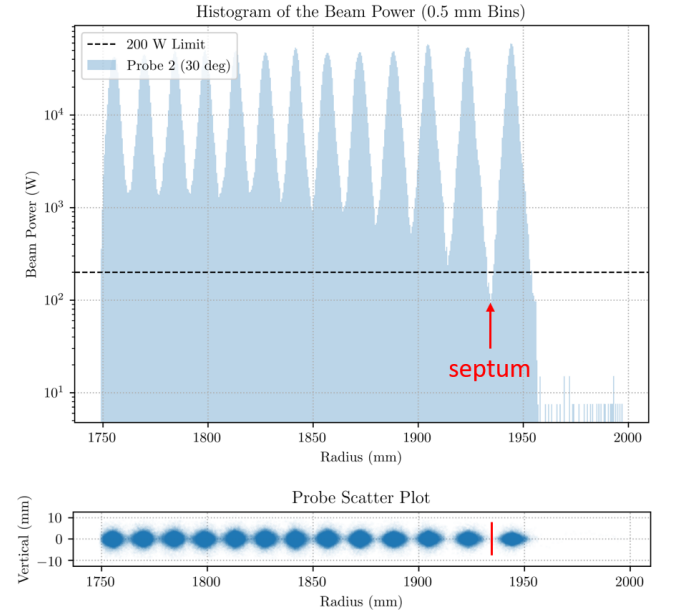


FIG. 16. Probe 2 (30°). The beam power binned in 0.5 mm bins (this is a conservative choice for septum width) versus radius (top). R-Z scatter plot of particles passing through the probe (bottom). It can be seen that a septum inserted at the right radial position would only take about 98 W of power.

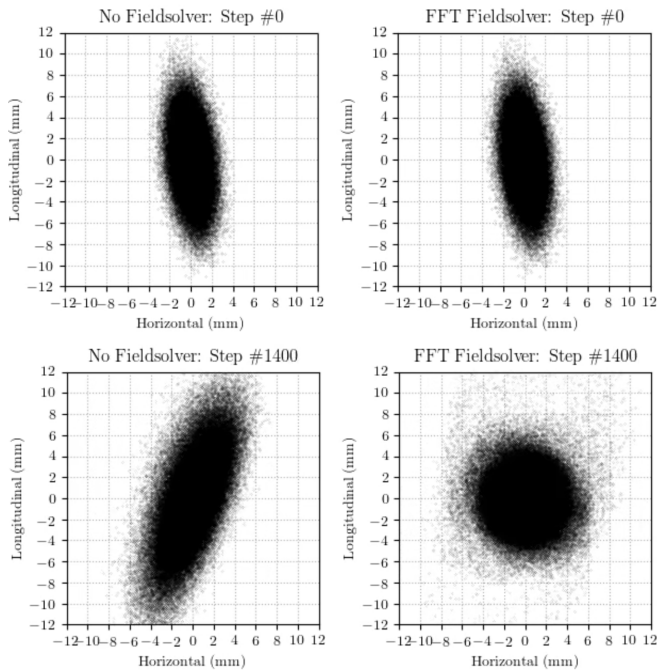


FIG. 17. Top: Starting bunch in local frame ('longitudinal' is the direction of the bunch mean momentum). Bottom: Bunches in local frame after 7 turns. No space-charge (left), space-charge for 6.65 mA (right). By coupling space-charge and external focusing, a round distribution with halo develops. Identical initial bunches were used.

cess to reach a stage where the beam is matched and halo removal becomes efficient (i.e. no new halo is generated). One can see an example of the bunch in local frame (longitudinal = direction of mean momentum, transverse \sim radial direction, both centered at 0) in Figure 17. There seems thus to be a balance between removing particles before their energy becomes high enough to activate parts of the cyclotron and late enough for vortex motion to have produced a matched distribution.

Another important point is the effect of the $\nu_r = 1$ resonance on the beam size. It can be seen in Figure 14 and Figure 15 that after 60 MeV/amu, the longitudinal beam size and halo parameter both increase exponentially. At the same time, the beam precession induced by the resonance is what leads to the good turn separation in the last turn. In the next step, a septum and appropriate electric field will be modelled and beam will be guided to, or even through a simple extraction channel to see how the beam quality (size, emittance, energy spread) changes during the extraction process.

A. Protecting the septum with a stripping foil

To mitigate beam loss on the septum, a new concept was introduced by collaborator Luciano Calabretta and has been discussed in the context of medical isotope production in [6]. The septum can be protected by placing

a shadow foil in front of it. This carbon foil intercepts particles that would otherwise hit the septum. H_2^+ ions are stripped of their electron and the resulting protons are extracted from the cyclotron and safely terminate in a beam dump. We estimate that about $\sim 0.02\%$ of the beam will be lost in this way, a number that is insignificant compared to the beam loss in the central region. The scheme is illustrated in Figure 18.

IV CONCLUSION

In this report, we summarized the IsoDAR 60 MeV/amu simulations using the particle-in-cell code OPAL. Early on, it was shown by Jianjun Yang that a beam, matched or mismatched, will eventually, through vortex motion, become approximately round ($x_{rms} \approx y_{rms}$). By placing collimators during the first several turns of acceleration, halo developing in the matching process can be removed in a controlled manner without activation of the machine. These simulations were then repeated and extended from a starting energy of 1.5 MeV/amu down to 0.193 MeV/amu (essentially the first turn) with similar results. Beam loss on these collimators varies between 10% and 25%, with power deposition on the septum around 100 W (half of the safety limit of 200 W determined at PSI). These are high fidelity simulations, using $1e5$ to $1e6$ particles per bunch. However, further sensitivity studies are still necessary to determine how the system will react to variations in input beam current and placement, as well as additional energy spread from the spiral inflector. In the meantime, we propose a mitigation method in which H_2^+ particles which would hit the septum are stripped of their remaining electron by means of a narrow foil. The resulting protons have reduced magnetic rigidity and will go on a different path, missing the septum. They have to be extracted from the cyclotron and safely dumped (or used for a different purpose).

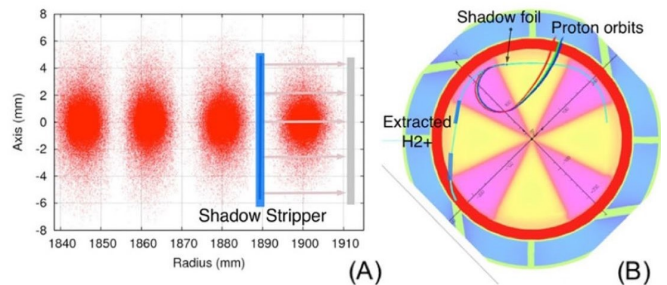


FIG. 18. (A) Placing a thin carbon foil intercepts particles that would otherwise hit the septum. These H_2^+ ions are stripped of their electron and the resulting protons are extracted from the cyclotron and safely terminate in a beam dump. From [6].

A. Outlook

All simulations of the IsoDAR cyclotron in this technical report were performed with harmonic 6. In the recent past, however, the collaboration has made the decision to switch to harmonic 4 and the simulations are currently repeated with the lower frequency. Preliminary results with a wider cavity opening angle of 42° show very similar results to the ones presented here for harmonic 6. This report will be updated in the near future to include the new results. The same holds for multi-bunch simulations, wherein OPAL injects five bunches in sequence (one per full turn for five turns) to account for the space

charge effect of neighboring bunches. The results are not dramatically changed. The final step will be to repeat the AIMA central region simulations with space-charge and use the output particle distribution as input in the OPAL IsoDAR 60 MeV/amu simulations.

V ACKNOWLEDGMENTS

This work has been supported by the Heising-Simons Foundation, and the US National Science Foundation under grants NSF-PA-1912764 and NSF-MRI-1626069.

-
- [1] A. Bungau, A. Adelmann, J. R. Alonso, W. Barletta, R. Barlow, L. Bartoszek, L. Calabretta, A. Calanna, D. Campo, J. M. Conrad, Z. Djurcic, Y. Kamyshev, M. H. Shaevitz, I. Shimizu, T. Smidt, J. Spitz, M. Wascko, L. A. Winslow, and J. J. Yang, *Phys. Rev. Lett.* **109**, 141802 (2012).
 - [2] A. Adelmann, J. R. Alonso, W. Barletta, R. Barlow, L. Bartoszek, A. Bungau, L. Calabretta, A. Calanna, D. Campo, J. M. Conrad, Z. Djurcic, Y. Kamyshev, H. Owen, M. H. Shaevitz, I. Shimizu, T. Smidt, J. Spitz, M. Touns, M. Wascko, L. A. Winslow, and J. J. Yang, *arxiv:1210.4454 [physics.acc-ph]* (2012).
 - [3] M. Abs, A. Adelmann, J. Alonso, S. Axani, W. Barletta, R. Barlow, L. Bartoszek, A. Bungau, L. Calabretta, *et al.*, *arXiv preprint arXiv:1511.05130* (2015).
 - [4] P. Schmor, in *Proceedings of CYCLOTRONS* (2010) pp. 419–424.
 - [5] J. R. Alonso, R. Barlow, J. M. Conrad, and L. H. Waites, *Nature Reviews Physics* **1**, 533 (2019).
 - [6] L. H. Waites, J. R. Alonso, R. Barlow, and J. M. Conrad, *EJNMMI Radiopharmacy and Chemistry* **5**, 6 (2020).
 - [7] Y. Ishi, M. Inoue, Y. Kuriyama, Y. Mori, T. Uesugi, J. Lagrange, T. Planche, M. Takashima, E. Yamakawa, H. Imazu, *et al.*, in *Proceedings of IPAC10, Kyoto* (2010) p. 1323.
 - [8] C. Rubbia, C. Roche, J. A. Rubio, F. Carminati, Y. Kadi, P. Mandrillon, J. P. C. Revol, S. Buono, R. Klapisch, N. Fiétier, *et al.*, *Conceptual design of a fast neutron operated high power energy amplifier*, Tech. Rep. (1995).
 - [9] J. Biarrotte, D. Uriot, F. Bouly, D. Vandeplasse, and J. Carneiro, in *Proceedings of SRF13* (2013).
 - [10] P. Lisowski, in *Proceedings of PAC97*, Vol. 97 (1997) p. 3780.
 - [11] J. Alonso, F. Avignone, W. Barletta, R. Barlow, H. Baumgartner, A. Bernstein, E. Blucher, L. Bugel, L. Calabretta, L. Camilleri, *et al.*, *arXiv preprint arXiv:1006.0260* (2010).
 - [12] C. Aberle, A. Adelmann, J. Alonso, W. Barletta, R. Barlow, L. Bartoszek, A. Bungau, A. Calanna, D. Campo, *et al.*, *arXiv preprint arXiv:1307.2949* (2013).
 - [13] M. Abs, A. Adelmann, J. Alonso, W. Barletta, R. Barlow, L. Calabretta, A. Calanna, D. Campo, L. Celona, J. Conrad, *et al.*, *arXiv preprint arXiv:1207.4895* (2012).
 - [14] L. Calabretta, L. Celona, S. Gammino, D. Rifuggiato, G. Ciavola, M. Maggiore, L. Piazza, J. Alonso, W. Barletta, *et al.*, *arXiv preprint arXiv:1107.0652* (2011).
 - [15] J. M. Conrad, D. Collaboration, *et al.*, *Nuclear Physics B-Proceedings Supplements* **229**, 386 (2012).
 - [16] D. Winklehner, J. Bahng, L. Calabretta, A. Calanna, A. Chakrabarti, J. Conrad, G. D’Agostino, S. Dechoudhury, V. Naik, L. Waites, *et al.*, *Nuclear Instruments and Methods in Physics Research Section A: Accelerators, Spectrometers, Detectors and Associated Equipment* **907**, 231 (2018).
 - [17] A. Moeslang, V. Heinzl, H. Matsui, and M. Sugimoto, *Fusion Engineering and Design Proceedings of the Seventh International Symposium on Fusion Nuclear Technology*, **81**, 863 (2006).
 - [18] K. W. Ehlers and K. N. Leung, *Review of Scientific Instruments* **54**, 677 (1983).
 - [19] M. Conjat and P. Mandrillon, *Central Region studies for the IsoDAR test cyclotron*, Tech. Rep. (AIMA Development, 2018).
 - [20] A. Calanna, D. Campo, J. J. Yang, L. Calabretta, D. Rifuggiato, M. M. Maggiore, L. A. C. Piazza, and A. Adelmann, in *Proceedings, 3rd International Conference on Particle accelerators (IPAC 2012)*, Vol. C1205201 (2012) pp. 424–426.
 - [21] J. Yang, A. Adelmann, W. Barletta, L. Calabretta, A. Calanna, D. Campo, and J. Conrad, *Nuclear Instruments and Methods in Physics Research Section A: Accelerators, Spectrometers, Detectors and Associated Equipment* **704**, 84 (2013).
 - [22] J. Jonnerby, *Central Region Design of a Compact High Intensity Cyclotron*, Master’s thesis, ETH Zürich, Switzerland (2016).
 - [23] C. Baumgarten, *Physical Review Special Topics-Accelerators and Beams* **14**, 114201 (2011).
 - [24] J. Yang, A. Adelmann, M. Humbel, M. Seidel, T. Zhang, *et al.*, *Physical Review Special Topics-Accelerators and Beams* **13**, 064201 (2010).
 - [25] A. Adelmann, A. Gsell, C. Kraus, Y. Ineichen, S. Russell, Y. Bi, C. Wang, J. Yang, H. Zha, S. Sheehy, C. Rogers, and C. Mayes, *The OPAL (Object Oriented Parallel Accelerator Library) Framework*, Tech. Rep. PSI-PR-08-02 (Paul Scherrer Institut, (2008-2015)).